

Catalysis-Induced Phase Separation and Autoregulation of Enzymatic Activity

Matthew W. Cotton,^{1,2} Ramin Golestanian,^{2,3,*} and Jaime Agudo-Canalejo^{2,†}

¹Mathematical Institute, University of Oxford, Woodstock Road, Oxford, OX2 6GG, United Kingdom

²Department of Living Matter Physics, Max Planck Institute for Dynamics and Self-Organization, D-37077 Göttingen, Germany

³Rudolf Peierls Centre for Theoretical Physics, University of Oxford, Oxford OX1 3PU, United Kingdom

(Dated: May 26, 2022)

We present a thermodynamically consistent model describing the dynamics of a multi-component mixture where one enzyme component catalyzes a reaction between other components. We find that the catalytic activity alone can induce phase separation for sufficiently active systems and large enzymes, without any equilibrium interactions between components. In the limit of fast reaction rates, binodal lines can be calculated using a mapping to an effective free energy. We also explain how this catalysis-induced phase separation (CIPS) can act to autoregulate the enzymatic activity, which points at the biological relevance of this phenomenon.

Introduction.—Liquid-liquid phase separation has emerged in recent years as a key principle governing intracellular organization [1, 2]. It is generally believed that the main drivers of phase separation in such systems are the attractive equilibrium interactions between the different soluble components, which are needed to overcome the entropic costs associated with phase separation [3, 4]. The emergence of condensates that are enriched or depleted in specific molecules can be designed by tuning these interactions [5–8]. On the other hand, it is clear that intracellular environments are far from being at thermodynamic equilibrium, and that the possible effects of non-equilibrium activity on phase separation need to be taken into consideration [9–15]. In all of these studies, however, equilibrium interactions have remained the driving force for phase separation; non-equilibrium effects have entered only as additional chemical reactions that convert the phase-separating components into each other [9–11] or, in a coarse-grained description, as gradients [11–13] or non-reciprocal [14, 15] terms that do not derive from a free energy. These non-equilibrium effects, albeit not driving the phase separation process, may for example affect the size distribution and coarsening dynamics of the resulting condensates, or lead to the formation of static and moving micropatterns.

Biomolecular condensates are often rich in enzymes that catalyze chemical reactions, in which case they are known as metabolons [16]. Such enzyme-rich condensates can also be assembled *in vitro* [17]. The packing of enzymes in close proximity to each other can cause changes in metabolic and enzymatic rates when compared to a homogeneous system, for example by substrate channelling, where an intermediate product in a cascade reaction is passed on between enzymes [18], or by mechanical effects that alter the catalytic rate [19]. Moreover, it has been suggested that biological systems can self-organize the cell cycle dynamics to lower the overall rate of metabolic activity and the ensuing free energy dissipation [20]. While the mechanisms underlying both the formation of enzyme-rich condensates and metabolic auto-regulation are currently not well understood [16, 20], it would be

interesting to investigate whether such behaviours can generically emerge from spatial organization that arises from catalysis-induced non-equilibrium activity.

Here, we propose a fundamentally new mechanism for the formation of enzyme-rich condensates, which does not rely on equilibrium attractive interactions between enzymes, but rather on effective interactions that arise purely as a consequence of their non-equilibrium catalytic activity (see Fig. 1 for a schematic of the phenomenon and Fig. 2 for the corresponding phase diagrams). While effective interactions mediated by self-generated chemical gradients have been previously described in the context of phoretic active colloids or chemotactic microorganisms [21–25], these were based on a microscopic and hydrodynamic description of individual colloid-colloid interactions. The theoretical framework presented here takes a complementary approach based on non-equilibrium thermodynamics and Flory-Huggins theory of suspensions, to manifestly connect the phenomenology to the existing studies on intracellular phase separation [3–10]. We find that this catalysis-induced phase separation (CIPS) can

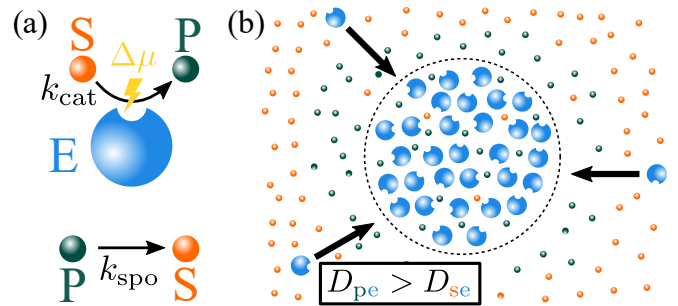


FIG. 1. Processes leading to catalysis-induced phase separation (CIPS). (a) Enzymes convert substrate into product by a fuelled catalytic reaction, while product turns into substrate spontaneously. (b) The catalyzed reaction creates gradients of substrate and product around enzyme-rich regions, which attract more enzymes when the off-diagonal transport coefficients coupling enzyme fluxes to product and substrate thermodynamic forces satisfy $D_{pe} > D_{se}$.

be described by a mapping to an effective free energy, and thus shows equilibrium features such as the existence of binodal and spinodal lines which meet at a critical point. Moreover, we show that phase separation in this model, which is itself induced by catalysis, generically leads to a decrease in the overall catalytic activity of the system, thus providing a mechanism for the autoregulation of catalytic activity.

Model.—We consider an incompressible fluid with N components described by the volume fractions $\phi_i(\mathbf{r}, t)$, each corresponding to individual molecules of volume v_i on the microscopic scale. The Flory-Huggins theory of suspensions gives the free energy of the system as $F = \int d\mathbf{r} f_{\text{FH}}$, with the free energy density $f_{\text{FH}}(\{\phi_i\}) = \sum_{i=1}^N \frac{1}{v_i} [\varepsilon_i \phi_i + k_B T \phi_i (\log \phi_i - 1)]$, where ε_i is the enthalpy of component i . Importantly, we consider components that only interact with each other through excluded volume effects and are otherwise non-interacting, i.e. f_{FH} does not contain terms of the form $\chi_{ij} \phi_i \phi_j$. This implies that phase separation in this system would be impossible at equilibrium. We denote $\beta \equiv (k_B T)^{-1}$. Each ϕ_i is governed by conserved dynamics $\dot{\phi}_i + \nabla \cdot \mathbf{J}_i = 0$ driven by thermodynamic fluxes $\mathbf{J}_i = -\sum_{j=1}^N M_{ij} \nabla \mu_j$, where $\mu_j = v_j \frac{\delta F}{\delta \phi_j} = \varepsilon_j + k_B T \log \phi_j$ is the chemical potential of component j , and M_{ij} is a mobility matrix [26]. Incompressibility of the suspension requires $\sum_{i=1}^N \phi_i = 1$, which implies (via the dynamical equations) that the mobilities must satisfy $\sum_i M_{ij} = 0$ [27]. The Onsager reciprocal relations further constrain the form of the mobilities, namely $v_i M_{ij} = v_j M_{ji}$ [26]. These constraints mean that a system of N components has $N(N-1)/2$ free mobilities. In the following, we assume the common form of $M_{ij} = -\beta D_{ij} \phi_i \phi_j$ for $i \neq j$, where the constraints just described imply $M_{jj} = -\sum_{i \neq j} M_{ij}$ and $v_i D_{ij} = v_j D_{ji}$ [6, 27–29]. We note that the single-particle transport coefficients D_{ij} represent the rate at which the components respond to local effective concentration gradients and exchange positions, and as such are inherently related to the phenomenon of diffusiophoresis [22]. In the absence of attractive interactions between the components, we have $D_{ij} > 0$.

We make the model active by allowing non-equilibrium (fuelled) conversion between two components, substrate (S) and product (P), catalyzed by an enzyme (E). This can be described by the reaction $E+S+F \rightleftharpoons E+P+W$, where F and W represent fuel and waste molecules, respectively. We do not model the dynamics of the fuel and waste here, but assume that the system is in contact with a reservoir that maintains constant chemical potentials, μ_f and μ_w , and define $\Delta\mu \equiv \mu_f - \mu_w$. Alternatively, $\Delta\mu$ could represent the energy transferred by a photon in a light-activated catalytic reaction. We further allow for spontaneous conversion between S and P, corresponding to the reaction $S \rightleftharpoons P$. Note that incompressibility implies $v_p = v_s$. Using the definition $\Delta\varepsilon \equiv \varepsilon_s - \varepsilon_p$, we can

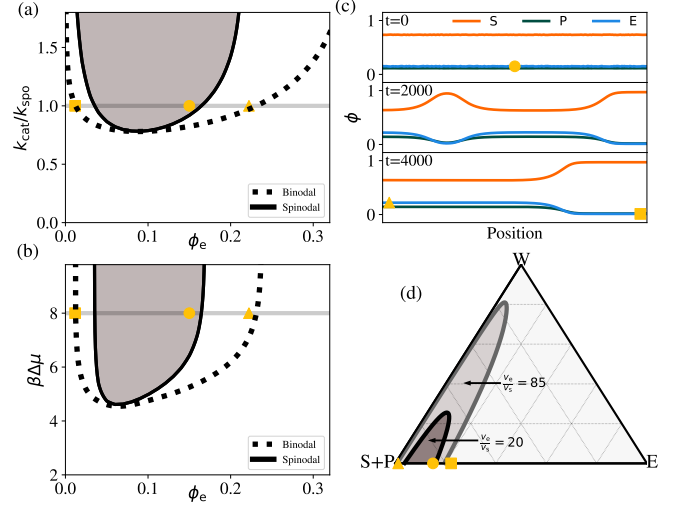


FIG. 2. Phase behaviour and onset of CIPS. (a,b) Spinodal lines [from (7)] and binodal lines (from the common tangent construction of f_{eff}) for (a) varying k_{cat} with $\Delta\mu = 8k_B T$ and (b) varying $\Delta\mu$ with $k_{\text{cat}}/k_{\text{spo}} = 1$. (c) Numerical simulations showing the evolution of a uniform steady state with $\phi_e = 0.15$ into two phase separated regions. The circle, triangle and square identify the homogeneous steady state and the dense and dilute enzyme phases, respectively, and are plotted in all other panels for comparison. (d) Stability diagram of a mixture including a water component, for $\Delta\mu = 8k_B T$ and $k_{\text{cat}}/k_{\text{spo}} = 1$. The darker and lighter shaded regions mark the spinodal regions for $v_e/v_s = 20$ [also used in (a–c)] and $v_e/v_s = 85$, respectively. Additional system parameters in (a–d) are $\Delta\varepsilon = -5k_B T$, $D_{pe} = 4D_{se}$, and $D_{ps} = 10D_{se}$; in (d) $D_{ew} = D_{sw} = D_{pw} = 10D_{se}$ and $v_w = v_s$.

write the net rate of the spontaneous reaction as

$$r_{\text{spo}} = r_{\text{spo}}^{\text{S} \rightarrow \text{P}} - r_{\text{spo}}^{\text{P} \rightarrow \text{S}} = k_{\text{spo}} [e^{\beta \Delta\varepsilon} \phi_s - \phi_p], \quad (1)$$

which entails detailed balance with $r_{\text{spo}}^{\text{S} \rightarrow \text{P}}/r_{\text{spo}}^{\text{P} \rightarrow \text{S}} = \exp[\beta(\mu_s - \mu_p)]$. The catalyzed reaction rate will have a similar functional form with an additional dependence on ϕ_e , namely

$$r_{\text{cat}} = r_{\text{cat}}^{\text{S} \rightarrow \text{P}} - r_{\text{cat}}^{\text{P} \rightarrow \text{S}} = k_{\text{cat}} \phi_e [\phi_s - \phi_p e^{-\beta(\Delta\varepsilon + \Delta\mu)}], \quad (2)$$

which also entails detailed balance with $r_{\text{cat}}^{\text{S} \rightarrow \text{P}}/r_{\text{cat}}^{\text{P} \rightarrow \text{S}} = \exp[\beta(\mu_s - \mu_p + \Delta\mu)]$. We will typically take $\Delta\varepsilon < 0$ and $\Delta\varepsilon + \Delta\mu > 0$, so that the spontaneous and catalyzed reactions run preferentially in the $\text{P} \rightarrow \text{S}$ and $\text{S} \rightarrow \text{P}$ directions, respectively; see Fig. 1. Combining the conserved dynamics with the reaction terms and defining $R \equiv r_{\text{spo}} + r_{\text{cat}}$ results in the evolution equations for the three-component system

$$\dot{\phi}_e = \nabla \cdot (M_{ee} \nabla \mu_e + M_{es} \nabla \mu_s + M_{ep} \nabla \mu_p), \quad (3)$$

$$\dot{\phi}_s = \nabla \cdot (M_{se} \nabla \mu_e + M_{ss} \nabla \mu_s + M_{sp} \nabla \mu_p) - R, \quad (4)$$

$$\dot{\phi}_p = \nabla \cdot (M_{pe} \nabla \mu_e + M_{ps} \nabla \mu_s + M_{pp} \nabla \mu_p) + R. \quad (5)$$

Steady-state and stability.—The minimal model [Eqs. (3)–(5)] has a homogeneous steady-state solution when $R = 0$, which is given by any ϕ_e^* as well as

$$\phi_s^* = \phi_{s+p}^* \frac{k_{\text{spo}} + k_{\text{cat}} \phi_e^* e^{-\beta(\Delta\varepsilon + \Delta\mu)}}{k_{\text{spo}} + k_{\text{cat}} \phi_e^* e^{-\beta(\Delta\varepsilon + \Delta\mu)} + k_{\text{spo}} e^{\beta\Delta\varepsilon} + k_{\text{cat}} \phi_e^*} \quad (6)$$

with $\phi_{s+p}^* = 1 - \phi_e^*$ and $\phi_p^* = \phi_{s+p}^* - \phi_s^*$.

We can study the linear stability of this homogeneous steady-state by considering a small perturbation $\phi_i(\mathbf{r}, t) = \phi_i^* + \delta\phi_i(\mathbf{r}, t)$. We find that the steady-state undergoes an instability at the longest wavelengths provided the following condition holds

$$\frac{1}{v_e \phi_e^*} + \frac{1}{v_s (1 - \phi_e^*)} < \frac{k_{\text{spo}} k_{\text{cat}} (1 - e^{-\beta\Delta\mu}) (D_{\text{pe}} - D_{\text{se}})}{v_s (R_s + R_p) (D_{\text{pe}} R_s + D_{\text{se}} R_p)}, \quad (7)$$

where we have defined $R_s \equiv k_{\text{spo}} e^{\beta\Delta\varepsilon} + k_{\text{cat}} \phi_e^*$ and $R_p \equiv k_{\text{spo}} + k_{\text{cat}} \phi_e^* e^{-\beta(\Delta\varepsilon + \Delta\mu)}$ [30]. Since the left hand side of (7) is always positive, an instability is possible only if the right hand side is positive as well. The sign of the right hand side is controlled by that of $(1 - e^{-\beta\Delta\mu}) (D_{\text{pe}} - D_{\text{se}})$, which has several implications. First, an equilibrium system with $\Delta\mu = 0$ is always stable. Second, for a catalytic reaction favouring product formation with $\Delta\mu > 0$, an instability is possible only if $D_{\text{pe}} > D_{\text{se}}$. Third, if $D_{\text{pe}} = D_{\text{se}}$ the system is always stable. Intuitively, the instability arises from opposing gradients of substrate and product generated around an enzyme-rich region when $\Delta\mu > 0$, coupled to an unequal response of the enzyme to gradients of substrate and product when $D_{\text{pe}} > D_{\text{se}}$, resulting in effective enzyme-enzyme attractive interactions and further aggregation. Interestingly, the instability is favoured when $v_e \gg v_s$, which happens to correspond to the typical relative sizes of enzymes and substrates in biological systems. In Fig. 2(a,b), the unstable region delimited by Eq. (7) is shown as a function of the catalytic rate k_{cat} and the non-equilibrium drive $\Delta\mu$.

Numerical solution of the evolution equations (3)–(5) confirms the existence of this instability. We initialize a 1D system with small number-conserving random variations around ϕ_i^* . When the system is unstable, regions of high and low enzyme concentrations develop spontaneously [see Fig. 2(c)] with the longer time dynamics leading to two distinct phase-separated domains, suggestive of the existence of a binodal line reminiscent of equilibrium phase separation.

Effective free energy and binodal.—In the macroscopic limit, we expect the substrate-product equilibrium in the bulk of each phase to be governed by the reaction terms that act locally, rather than by spatial diffusion. This implies that the substrate and product concentrations are enslaved to the enzyme concentration by $\phi_s \approx \phi_s^*(\phi_e)$ and $\phi_p \approx \phi_p^*(\phi_e)$, with the functions defined in (6). Substituting these expressions into (3), we can recast the dynamics of the enzyme as $\dot{\phi}_e \approx \nabla \cdot (M_{\text{ee}} \nabla \mu_{\text{eff}})$ with an

effective chemical potential for the enzyme

$$\frac{\mu_{\text{eff}}(\phi_e)}{k_{\text{B}}T} = \log \phi_e - \frac{v_e}{v_s} \log [D_{\text{es}} \phi_s^*(\phi_e) + D_{\text{ep}} \phi_p^*(\phi_e)]. \quad (8)$$

We can also identify an effective free energy density $f_{\text{eff}}(\phi_e)$, such that $\mu_{\text{eff}} = v_e \frac{df_{\text{eff}}}{d\phi_e}$, which can be explicitly calculated by direct integration [30]. By employing the common-tangent construction in unstable cases, we can identify two coexisting phases and define the binodal lines, which show good agreement with our numerical results and meet the spinodal line at a critical point; see Fig. 2(a,b).

The role of solvent.—While we have so far considered an enzyme-substrate-product system for simplicity, we observe that an instability can also occur in the presence of an additional solvent, typically water, in which these components will be dissolved. We can add a fourth component of volume fraction ϕ_w to the dynamics and study the stability of the homogeneous steady-state [30]. We find that the uniform steady-state can be unstable even when all the solute components (enzyme, substrate, and product) are in dilute conditions, as shown in Fig. 2(d). This demonstrates the wide reach of this work and its potential application to realistic systems. For the remainder of this Letter, however, we focus on the simpler $\phi_w = 0$ case.

Enzymatic autoregulation.—A biologically pertinent question is what happens to the enzymatic activity when the system phase separates. The average rate of catalysis in a region of size L is given by $\bar{r}_{\text{cat}} = \frac{1}{L} \int_0^L r_{\text{cat}} dx$ in a simple 1D case. In a homogeneous state, r_{cat} will be constant throughout the system and, using Eq. (2), will go as $\bar{r}_{\text{cat}}^{(h)} \sim \phi_e (1 - \phi_e)$ which is a concave function of ϕ_e . In a phase separated state, \bar{r}_{cat} is a weighted average of the catalytic rates in each phase, with the weights determined by the lever rule. Due to the concavity of $\bar{r}_{\text{cat}}^{(h)}$, we find that the catalytic rate in the phase separated state is always smaller than in the homogeneous state; see Fig. 3(a). We observe a similar behaviour when we vary a control parameter such as $\Delta\mu$, which is controlled by the concentration of the fuel molecules in an experiment; see Fig. 3(b). In the homogeneous phase, \bar{r}_{cat} initially rises and then saturates with increasing $\Delta\mu$. The phase separation reduces \bar{r}_{cat} in the whole system and leads to saturation at a lower activity. Through this mechanism, CIPS can act to autoregulate the enzymatic activity of the mixture: once the activity reaches a threshold, the system phase separates and gives rise to a reduced overall catalytic rate. A similar saturation effect is seen when other system parameters, such as k_{cat} , are varied causing the system to phase separate.

Discussion.—Using a thermodynamically-consistent description of a multicomponent fluid based on linear response theory constructed from a Flory-Huggins free energy, we have identified a new, purely non-equilibrium

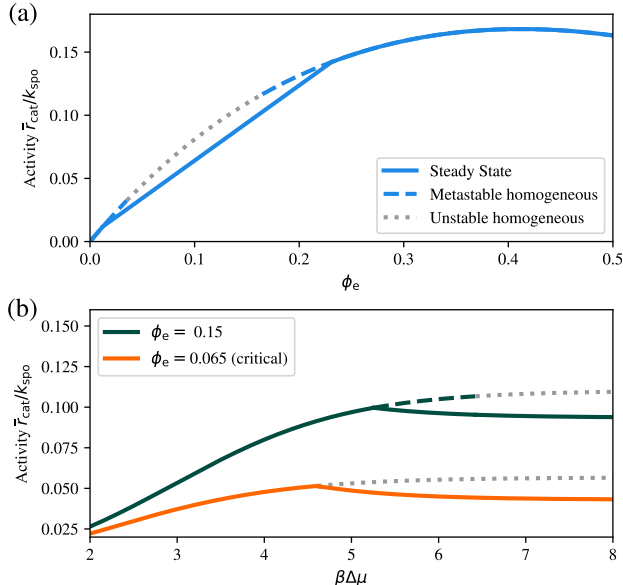


FIG. 3. Effect of CIPS on catalytic activity. (a) Activity as a function of the initial ϕ_e . In the phase separated state, the activity is a linear combination of the activity of the homogeneous states on either side of the binodal, which due to convexity is always smaller than that of the homogeneous state. (b) Evolution of activity with increasing $\Delta\mu$. As the system phase separates, the overall catalytic rate is reduced. When $\phi_e = 0.065$, the system passes through the critical point and there is no metastable homogeneous branch. System parameters are as in Fig. 2.

mechanism for phase separation as a consequence of the catalytic, fuelled conversion between two components (substrate and product) by a third component (enzyme). Besides the catalytic activity, a necessary ingredient for catalysis-induced phase separation (CIPS) is an asymmetry in the off-diagonal response coefficients (mobilities) that couple enzyme-substrate and enzyme-product thermodynamic forces and fluxes in the non-equilibrium conserved dynamics. Using a mapping of the three-component system to a single-component system with an effective free energy, equilibrium-like features of CIPS such as binodal lines were obtained.

The mechanism behind CIPS is reminiscent of mechanisms for chemotactic or phoretic aggregation previously described in the literature in the context of interacting microorganisms or catalytically-active colloids [21–23, 25]. However, these studies were based on microscopic descriptions of the chemotactic or phoretic response, typically valid only under dilute conditions. We expect that such microscopic descriptions and the thermodynamic-phenomenological description presented here are two sides of the same coin, the former being applicable arbitrarily far from equilibrium in dilute condi-

tions, the latter near equilibrium at arbitrary densities. Future work may thus explore the connection between microscopic parameters in phoretic-chemotactic theories and the phenomenological mobility coefficients M_{ij} describing the non-equilibrium linear response.

When the enzymatic activity in the homogeneous system is increased beyond a critical threshold, for example via external factors such as the availability of fuel molecules, the system phase separates, causing the overall enzymatic activity of the system to suddenly decrease and then plateau. This makes CIPS a novel mechanism for the autoregulation of single-step catalytic reactions. It remains to be seen how CIPS affects catalytic activity in multi-step metabolic reactions involving several distinct enzymes. We speculate that, in a system with several enzyme components, CIPS may allow for colocalization of distinct enzymes within the same aggregate, allowing for substrate channelling as in cellular metabolons [16, 18]. Indeed, we previously showed that this behaviour is possible in mixtures of phoretic active colloids [23].

In order to highlight that catalytic activity alone is enough to induce phase separation, we considered here a system with excluded volume interactions only. One may naturally incorporate the usual equilibrium interaction terms (e.g. $\chi_{ij}\phi_i\phi_j$ and $\kappa_{ij}\nabla\phi_i\cdot\nabla\phi_j$) into f_{FH} , and explore the competition or cooperation between equilibrium interactions and non-equilibrium catalytic effective interactions in phase separation. In particular, we note that we have focused here on effective interactions that are attractive, i.e. those with $(1 - e^{-\beta\Delta\mu})(D_{\text{pe}} - D_{\text{se}}) > 0$ so that the right hand side of (7) is positive. One may also consider repulsive effective interactions, with $(1 - e^{-\beta\Delta\mu})(D_{\text{pe}} - D_{\text{se}}) < 0$. In this case, we expect that an enzyme-rich condensate held together by equilibrium interactions may be *dissolved* by sufficiently strong non-equilibrium catalytic activity. This further highlights how the mechanism we have uncovered goes well beyond the prototypical example presented here, and may prove an important player in the description of phase separation in out-of-equilibrium systems.

This work has received support from the Max Planck School Matter to Life and the MaxSynBio Consortium, which are jointly funded by the Federal Ministry of Education and Research (BMBF) of Germany, and the Max Planck Society. M.C. was supported by funding from the Biotechnology and Biological Sciences Research Council (UKRI-BBSRC) [grant number BB/T008784/1].

* ramin.golestanian@ds.mpg.de

† jaime.agudo@ds.mpg.de

[1] S. F. Banani, H. O. Lee, A. A. Hyman, and M. K. Rosen, Biomolecular condensates: organizers of cellular biochemistry, *Nat. Rev. Mol. Cell Biol* **18**, 285 (2017).

- [2] Y. Shin and C. P. Brangwynne, Liquid phase condensation in cell physiology and disease, *Science* **357**, eaaf4382 (2017).
- [3] C. P. Brangwynne, P. Tompa, and R. V. Pappu, Polymer physics of intracellular phase transitions, *Nat. Phys.* **11**, 899 (2015).
- [4] J. Berry, C. P. Brangwynne, and M. Haataja, Physical principles of intracellular organization via active and passive phase transitions, *Rep. Prog. Phys.* **81**, 046601 (2018).
- [5] S. Mao, D. Kuldinow, M. P. Haataja, and A. Košmrlj, Phase behavior and morphology of multicomponent liquid mixtures, *Soft Matter* **15**, 1297 (2019).
- [6] S. Mao, M. S. Chakraverti-Wuerthwein, H. Gaudio, and A. Košmrlj, Designing the morphology of separated phases in multicomponent liquid mixtures, *Phys. Rev. Lett.* **125**, 218003 (2020).
- [7] W. M. Jacobs, Self-Assembly of Biomolecular Condensates with Shared Components, *Phys. Rev. Lett.* **126**, 258101 (2021).
- [8] K. Shrinivas and M. P. Brenner, Phase separation in fluids with many interacting components, *Proc. Natl. Acad. Sci. U.S.A.* **118**, e2108551118 (2021).
- [9] C. A. Weber, D. Zwicker, F. Jülicher, and C. F. Lee, Physics of active emulsions, *Rep. Prog. Phys.* **82**, 064601 (2019).
- [10] J. Kirschbaum and D. Zwicker, Controlling biomolecular condensates via chemical reactions, *J. R. Soc. Interface* **18**, 20210255.
- [11] Y. I. Li and M. E. Cates, Non-equilibrium phase separation with reactions: A canonical model and its behaviour, *J. Stat. Mech.: Theory Exp.* **2020** (5), 053206.
- [12] R. Wittkowski, A. Tiribocchi, J. Stenhammar, R. J. Allen, D. Marenduzzo, and M. E. Cates, Scalar φ^4 field theory for active-particle phase separation, *Nat. Commun.* **5**, 4351 (2014).
- [13] E. Tjhung, C. Nardini, and M. E. Cates, Cluster phases and bubbly phase separation in active fluids: reversal of the ostwald process, *Phys. Rev. X* **8**, 031080 (2018).
- [14] S. Saha, J. Agudo-Canalejo, and R. Golestanian, Scalar active mixtures: The nonreciprocal cahn-hilliard model, *Phys. Rev. X* **10**, 041009 (2020).
- [15] Z. You, A. Baskaran, and M. C. Marchetti, Nonreciprocity as a generic route to traveling states, *Proc. Natl. Acad. Sci. U.S.A.* **117**, 19767 (2020).
- [16] L. J. Sweetlove and A. R. Fernie, The role of dynamic enzyme assemblies and substrate channelling in metabolic regulation, *Nat. Commun.* **9**, 2136 (2018).
- [17] A. Testa, M. Dindo, A. A. Rebane, B. Nasouri, R. W. Style, R. Golestanian, E. R. Dufresne, and P. Laurino, Sustained enzymatic activity and flow in crowded protein droplets, *Nat. Commun.* **12**, 6293 (2021).
- [18] L. Poshyvailo, E. von Lieres, and S. Kondrat, Does metabolite channeling accelerate enzyme-catalyzed cascade reactions?, *PLOS ONE* **12**, e0172673 (2017).
- [19] J. Agudo-Canalejo, T. Adeleke-Larodo, P. Illien, and R. Golestanian, Synchronization and enhanced catalysis of mechanically coupled enzymes, *Phys. Rev. Lett.* **127**, 208103 (2021).
- [20] B. Niebel, S. Leupold, and M. Heinemann, An upper limit on gibbs energy dissipation governs cellular metabolism, *Nat. Metab.* **1**, 125 (2019).
- [21] S. Saha, R. Golestanian, and S. Ramaswamy, Clusters, asters, and collective oscillations in chemotactic colloids, *Phys. Rev. E* **89**, 062316 (2014).
- [22] R. Golestanian, Phoretic active matter, arXiv:1909.03747.
- [23] J. Agudo-Canalejo and R. Golestanian, Active Phase Separation in Mixtures of Chemically Interacting Particles, *Phys. Rev. Lett.* **123**, 018101 (2019).
- [24] B. Nasouri and R. Golestanian, Exact phoretic interaction of two chemically active particles, *Phys. Rev. Lett.* **124**, 168003 (2020).
- [25] E. F. Keller and L. A. Segel, Initiation of slime mold aggregation viewed as an instability, *J. Theor. Biol.* **26**, 399 (1970).
- [26] S. R. de Groot and P. Mazur, *Non-Equilibrium Thermodynamics* (Dover publ, New York, 1984).
- [27] K. Kehr, K. Binder, and S. Reulein, Mobility, interdiffusion, and tracer diffusion in lattice-gas models of two-component alloys, *Phys. Rev. B* **39**, 4891 (1989).
- [28] E. J. Kramer, P. Green, and C. J. Palmström, Interdiffusion and marker movements in concentrated polymer-polymer diffusion couples, *Polymer* **25**, 473 (1984).
- [29] S. Bo, L. Hubatsch, J. Bauermann, C. A. Weber, and F. Jülicher, Stochastic dynamics of single molecules across phase boundaries, *Phys. Rev. Res.* **3**, 043150 (2021).
- [30] See Supplemental Material at [URL will be inserted by publisher] for details on the calculation of the instability condition in the absence and presence of solvent, and the explicit expression for the effective free energy.

Supplemental Material: Catalysis-Induced Phase Separation and Autoregulation of Enzymatic Activity

STABILITY OF THE THREE-COMPONENT SYSTEM

Condition of instability

We consider the stability of the homogeneous steady state of a three component mixture described by volume fractions ϕ_e^* , ϕ_s^* and ϕ_p^* which satisfy $R = 0$. We consider a small perturbation from this uniform steady state $\phi_i(\mathbf{r}, t) = \phi_i^* + \delta\phi_i(\mathbf{r}, t)$ giving $\mu_i(\mathbf{r}, t) = \mu_i^* + \delta\mu_i(\mathbf{r}, t)$ and define mobilities at the homogeneous steady state $M_{ij}^* = M_{ij}(\phi_e^*, \phi_s^*, \phi_p^*)$. To first order in the perturbation $\delta\mu(\mathbf{r}, t) = \frac{\delta\phi_i(\mathbf{r}, t)}{\phi_i^*}$ and thus $\nabla\mu_i(\mathbf{r}, t) = \frac{1}{\phi_i^*}\nabla\delta\phi_i(\mathbf{r}, t)$, and moreover $R = R_s\delta\phi_s - R_p\delta\phi_p + R_e\delta\phi_e$ where $R_s = k_{\text{spo}}e^{\beta\Delta\varepsilon} + k_{\text{cat}}\phi_e^*$ and $R_p = k_{\text{spo}} + k_{\text{cat}}\phi_e^*e^{-\beta(\Delta\varepsilon+\Delta\mu)}$ as defined in the main text, and

$$R_e \equiv k_{\text{cat}}[\phi_s^* - \phi_p^*e^{-\beta(\Delta\varepsilon+\Delta\mu)}] = \phi_{s+p}^* \frac{k_{\text{cat}}k_{\text{spo}}(1 - e^{-\beta\Delta\mu})}{k_{\text{spo}} + k_{\text{cat}}\phi_e^*e^{-\beta(\Delta\varepsilon+\Delta\mu)} + k_{\text{spo}}e^{\beta\Delta\varepsilon} + k_{\text{cat}}\phi_e^*}. \quad (\text{S1})$$

The governing equations for the perturbations $\delta\phi_i(\mathbf{q}, t)$ in Fourier space are found as follows

$$\begin{pmatrix} \delta\dot{\phi}_e \\ \delta\dot{\phi}_s \\ \delta\dot{\phi}_p \end{pmatrix} = \underbrace{\begin{pmatrix} (M_{\text{se}}^* + M_{\text{pe}}^*)\frac{\mathbf{q}^2}{\phi_e^*} & -M_{\text{se}}^*\frac{v_e}{v_s}\frac{\mathbf{q}^2}{\phi_s^*} & -M_{\text{pe}}^*\frac{v_e}{v_s}\frac{\mathbf{q}^2}{\phi_p^*} \\ -M_{\text{se}}^*\frac{\mathbf{q}^2}{\phi_e^*} - R_e & (M_{\text{sp}}^* + M_{\text{se}}^*\frac{v_e}{v_s})\frac{\mathbf{q}^2}{\phi_s^*} - R_s & -M_{\text{sp}}^*\frac{\mathbf{q}^2}{\phi_p^*} + R_p \\ -M_{\text{pe}}^*\frac{\mathbf{q}^2}{\phi_e^*} + R_e & -M_{\text{sp}}^*\frac{\mathbf{q}^2}{\phi_s^*} + R_s & (M_{\text{pe}}^*\frac{v_e}{v_s} + M_{\text{sp}}^*)\frac{\mathbf{q}^2}{\phi_p^*} - R_p \end{pmatrix}}_{\mathcal{C}} \begin{pmatrix} \delta\phi_e \\ \delta\phi_s \\ \delta\phi_p \end{pmatrix}.$$

In this formulation, we can explicitly see the incompressibility being imposed as the columns of \mathcal{C} sum to zero. We now eliminate one of the components, e.g. $\delta\phi_p = -\delta\phi_e - \delta\phi_s$, and define a 2×2 matrix, \mathcal{K} , describing the evolution of the remaining components. This is obtained from \mathcal{C} by subtracting the last column from the other two (i.e. $\mathcal{K}_{ij} = \mathcal{C}_{ij} - \mathcal{C}_{i3}$ for $i, j \in \{1, 2\}$), giving

$$\begin{pmatrix} \delta\dot{\phi}_e \\ \delta\dot{\phi}_s \end{pmatrix} = \underbrace{\begin{pmatrix} (M_{\text{se}}^* + M_{\text{pe}}^*)\frac{\mathbf{q}^2}{\phi_e^*} + M_{\text{pe}}^*\frac{v_e}{v_s}\frac{\mathbf{q}^2}{\phi_p^*} & -M_{\text{se}}^*\frac{v_e}{v_s}\frac{\mathbf{q}^2}{\phi_s^*} + M_{\text{pe}}^*\frac{v_e}{v_s}\frac{\mathbf{q}^2}{\phi_p^*} \\ -M_{\text{se}}^*\frac{\mathbf{q}^2}{\phi_e^*} - R_e + M_{\text{sp}}^*\frac{\mathbf{q}^2}{\phi_p^*} - R_p & (M_{\text{sp}}^* + M_{\text{se}}^*\frac{v_e}{v_s})\frac{\mathbf{q}^2}{\phi_s^*} - R_s + M_{\text{sp}}^*\frac{\mathbf{q}^2}{\phi_p^*} - R_p \end{pmatrix}}_{\mathcal{K}} \begin{pmatrix} \delta\phi_e \\ \delta\phi_s \end{pmatrix}.$$

The eigenvalues of \mathcal{K} determine the stability of the steady state. The system is stable if and only if all eigenvalues of \mathcal{K} are negative. The Onsager relations and the non-negativity of R_i mean $\mathcal{K}_{1,1}$ and $\mathcal{K}_{2,2}$ are always negative, so $\text{tr}(\mathcal{K}) < 0$ and there is therefore one positive eigenvalue if $\det(\mathcal{K}) < 0$. The instability condition then becomes

$$\begin{aligned} & \left((M_{\text{se}}^* + M_{\text{pe}}^*)\frac{\mathbf{q}^2}{\phi_e^*} + M_{\text{pe}}^*\frac{v_e}{v_s}\frac{\mathbf{q}^2}{\phi_p^*} \right) \left((M_{\text{sp}}^* + M_{\text{se}}^*\frac{v_e}{v_s})\frac{\mathbf{q}^2}{\phi_s^*} - R_s + M_{\text{sp}}^*\frac{\mathbf{q}^2}{\phi_p^*} - R_p \right) \\ & < \left(-M_{\text{se}}^*\frac{v_e}{v_s}\frac{\mathbf{q}^2}{\phi_s^*} + M_{\text{pe}}^*\frac{v_e}{v_s}\frac{\mathbf{q}^2}{\phi_p^*} \right) \left(-M_{\text{se}}^*\frac{\mathbf{q}^2}{\phi_e^*} - R_e + M_{\text{sp}}^*\frac{\mathbf{q}^2}{\phi_p^*} - R_p \right). \end{aligned} \quad (\text{S4})$$

When \mathbf{q} is very large, we expect the system to be stable as in this regime the evolution is dominated by diffusive relaxation. For $\mathbf{q} = 0$, the system is at critical stability due to global conservation, as this corresponds to a uniform change in ϕ_i . As such, since this condition only depends on \mathbf{q}^2 and \mathbf{q}^4 , the instability is satisfied if and only if it is satisfied for very small \mathbf{q}^2 . With this in mind we take Eq. (S4) to order $\sim \mathbf{q}^2$ which gives

$$\frac{1}{v_e\phi_e^*} + \frac{1}{v_s(1 - \phi_e^*)} < \frac{R_e}{v_s(1 - \phi_e^*)} \left(\frac{\gamma_p}{R_s} - \frac{\gamma_s}{R_p} \right) \quad (\text{S5})$$

where we have defined

$$\gamma_s \equiv \frac{M_{se}^*}{M_{se}^* + M_{pe}^*} \quad \text{and} \quad \gamma_p \equiv \frac{M_{pe}^*}{M_{se}^* + M_{pe}^*}. \quad (\text{S6})$$

This condition can also be written to constrain the relative volumes in the system

$$\frac{v_s}{v_e} < \frac{\phi_e^*}{1 - \phi_e^*} \left[R_e \left(\frac{\gamma_p}{R_s} - \frac{\gamma_s}{R_p} \right) - 1 \right], \quad (\text{S7})$$

which shows that the instability is favoured by larger enzymes, as stated in the main text. Assuming the following form for the mobility $M_{se} = -\beta D_{se} \phi_e \phi_s$ and $M_{pe} = -\beta D_{pe} \phi_e \phi_p$, gives

$$\frac{1}{v_e \phi_e^*} + \frac{1}{v_s (1 - \phi_e^*)} < \frac{R_e}{v_s (1 - \phi_e^*)} \frac{D_{pe} - D_{se}}{D_{pe} R_s + D_{se} R_p}. \quad (\text{S8})$$

which corresponds to the instability condition given in the main text. In calculating this condition, we eliminated the product component from the system and determined the stability by considering the other two components. Eliminating either of the other components gives the same result.

Fast dynamics

In deriving the stability condition for the minimal active mixture, we note that the eigenvalues of a 2×2 matrix can be given in terms of its trace, T and determinant, D , as $\lambda_{\pm} = \frac{1}{2}(T \pm \sqrt{T^2 + 4D})$. Alternatively, given the larger size of the enzymes, we could have made the assumption of fast substrate and product dynamics in comparison to the enzyme dynamics. Assuming that product and substrate equilibrate quickly, we can solve for $\delta \dot{\phi}_s = 0$ to find a relationship between $\delta \phi_s$ and $\delta \phi_e$. This gives

$$\delta \dot{\phi}_s = \mathcal{K}_{21} \delta \phi_e + \mathcal{K}_{22} \delta \phi_s = 0 \implies \delta \phi_s = -\frac{\mathcal{K}_{21}}{\mathcal{K}_{22}} \delta \phi_e \implies \delta \dot{\phi}_e = \mathcal{K}_{11} \delta \phi_e - \mathcal{K}_{12} \frac{\mathcal{K}_{21}}{\mathcal{K}_{22}} \delta \phi_e \quad (\text{S9})$$

and the instability condition then becomes

$$\mathcal{K}_{11} - \mathcal{K}_{12} \frac{\mathcal{K}_{21}}{\mathcal{K}_{22}} > 0. \quad (\text{S10})$$

Looking at the form of \mathcal{K}_{22} , in the small \mathbf{q} limit, $\mathcal{K}_{22} = -(R_s + R_p) < 0$, which gives

$$\mathcal{K}_{11} \mathcal{K}_{22} - \mathcal{K}_{21} \mathcal{K}_{12} < 0 \quad (\text{S11})$$

which is that $\det[\mathcal{K}] < 0$, the same condition in equation (S4). We subsequently use this slow enzyme assumption when dealing with enzymes and other interacting, fast components.

STABILITY OF THE FOUR-COMPONENT SYSTEM

An additional solvent component (e.g. water) can be added to the system similarly to the enzyme component, with conserved dynamics and no reaction terms. Following a similar procedure as for the no-solvent case, we can expand around a steady state where we now have $\phi_{s+p}^* \neq 1 - \phi_E^*$ but $\phi_w^* = 1 - \phi_{s+p}^* - \phi_E^*$. We can eliminate the solvent volume fraction to give a 3×3 matrix describing the evolution of E, S, and P volume fractions

$$(\delta \dot{\phi}_e, \delta \dot{\phi}_s, \delta \dot{\phi}_p)^T = \mathcal{K}_w (\delta \phi_e, \delta \phi_s, \delta \phi_p)^T \quad (\text{S12})$$

with

$$\mathcal{K}_w = \begin{pmatrix} (M_{se}^* + M_{pe}^* + M_{we}^*) \frac{q_e^2}{\phi_e^*} + M_{we}^* \frac{v_e}{v_w} \frac{q_w^2}{\phi_w^*} & -M_{se}^* \frac{v_e}{v_s} \frac{q_s^2}{\phi_s^*} + M_{we}^* \frac{v_e}{v_w} \frac{q_w^2}{\phi_w^*} & -M_{pe}^* \frac{v_e}{v_p} \frac{q_p^2}{\phi_p^*} + M_{we}^* \frac{v_e}{v_w} \frac{q_w^2}{\phi_w^*} \\ -M_{se}^* \frac{q_e^2}{\phi_e^*} - R_e + M_{ws}^* \frac{v_s}{v_w} \frac{q_w^2}{\phi_w^*} & (M_{se}^* \frac{v_e}{v_s} + M_{sp}^* + M_{ws}^*) \frac{q_s^2}{\phi_s^*} - R_s + M_{ws}^* \frac{v_s}{v_w} \frac{q_w^2}{\phi_w^*} & -M_{sp}^* \frac{q_p^2}{\phi_p^*} + R_p + M_{ws}^* \frac{v_s}{v_w} \frac{q_w^2}{\phi_w^*} \\ -M_{pe}^* \frac{q_e^2}{\phi_e^*} + R_e + M_{wp}^* \frac{v_s}{v_w} \frac{q_w^2}{\phi_w^*} & -M_{sp}^* \frac{q_s^2}{\phi_s^*} + R_s + M_{wp}^* \frac{v_s}{v_w} \frac{q_w^2}{\phi_w^*} & (M_{pe}^* \frac{v_e}{v_s} + M_{sp}^* + M_{wp}^*) \frac{q_p^2}{\phi_p^*} - R_p + M_{wp}^* \frac{v_s}{v_w} \frac{q_w^2}{\phi_w^*} \end{pmatrix}$$

We now assume that the substrate and product dynamics are fast in comparison to the enzyme. Setting $\delta\dot{\phi}_s = \delta\dot{\phi}_p = 0$ gives

$$\delta\dot{\phi}_e = (\mathcal{K}_w^{-1})_{1,1}\delta\phi_e \quad (\text{S14})$$

and so the system is unstable when

$$(\mathcal{K}_w^{-1})_{1,1} = \frac{(\mathcal{K}_w)_{2,2}(\mathcal{K}_w)_{3,3} - (\mathcal{K}_w)_{2,3}(\mathcal{K}_w)_{3,2}}{\det(\mathcal{K}_w)} \geq 0. \quad (\text{S15})$$

The numerator of (S15) is, to order \mathbf{q}^2 ,

$$\mathbf{q}^2 \left[-R_p \frac{M_{se}^* \frac{v_e}{v_s} + M_{ws}^*}{\phi_s^*} - R_s \frac{M_{pe}^* \frac{v_e}{v_s} + M_{wp}^*}{\phi_p^*} - \frac{v_s}{v_w \phi_w^*} (R_s + R_p) (M_{ws}^* + M_{wp}^*) \right]. \quad (\text{S16})$$

With the common choice of mobilities, $M_{ij} < 0$ for $i \neq j$, and $R_i \geq 0$, the expression (S16) is positive and the instability condition is simply

$$\det(\mathcal{K}_w) > 0, \quad (\text{S17})$$

which marks the transition from having all negative eigenvalues to having two negative and one positive eigenvalue. This expression is used to derive the instability (spinodal) line in Fig. 2(d) of the main text.

The determinant of \mathcal{K}_w has many terms and even when truncated to order \mathbf{q}^2 it is not a manageable expression. A key observation is that in the low solvent limit ($\phi_w \rightarrow 0$), and assuming Kramer's form for the mobilities, we recover the no-solvent case, as can be seen in Fig. 2(d) in the main text.

EFFECTIVE FREE ENERGY FOR THE THREE-COMPONENT SYSTEM

The effective free energy density f_{eff} can be determined by integration of μ_{eff} , such that $f_{\text{eff}}(\phi_e) = (1/v_e) \int \mu_{\text{eff}}(\phi_e) d\phi_e$. Since μ_{eff} can be determined up to a constant term, f_{eff} can be determined up to addition of an affine function in ϕ_e . The integration gives

$$\begin{aligned} \frac{f_{\text{eff}}(\phi_e)}{k_B T} &= \frac{1}{v_p} \frac{k_{\text{spo}}}{k_{\text{cat}}} \left(\frac{1 + e^{\beta \Delta \varepsilon}}{1 + e^{-\beta(\Delta \varepsilon + \Delta \mu)}} \log \left[\frac{k_{\text{cat}}}{k_{\text{spo}}} \phi_e + e^{\beta(\Delta \varepsilon + \Delta \mu)} \left(1 + e^{\beta \Delta \varepsilon} + \frac{k_{\text{cat}}}{k_{\text{spo}}} \phi_e \right) \right] \right. \\ &\quad \left. - \frac{D_{se} + D_{pe} e^{\beta \Delta \varepsilon}}{D_{pe} + D_{se} e^{-\beta(\Delta \varepsilon + \Delta \mu)}} \log \left[D_{se} \frac{k_{\text{cat}}}{k_{\text{spo}}} \phi_e + e^{\beta(\Delta \varepsilon + \Delta \mu)} (D_{se} + D_{pe} e^{\beta \Delta \varepsilon} + D_{pe} \frac{k_{\text{cat}}}{k_{\text{spo}}} \phi_e) \right] \right) \\ &\quad + \left(\frac{1}{v_p} - \frac{1}{v_e} \right) \phi_e + \frac{1}{v_p} \log[1 - \phi_e] + \phi_e \left(\frac{1}{v_e} \log \phi_e - \frac{1}{v_p} \log[D_{es} \phi_s^*(\phi_e) + D_{ep} \phi_p^*(\phi_e)] \right), \end{aligned} \quad (\text{S18})$$

which, together with μ_{eff} , was used for the calculation of the binodal lines in Fig. 2(a,b) using the Maxwell construction.